Earth and Planetary Science Letters 297 (2010) 405–412

Contents lists available at ScienceDirect

Earth and Planetary Science Letters

journal homepage: www.elsevier.com/locate/epsl

Subduction of continental lithosphere in the Banda Sea region: Combining evidence from full waveform tomography and isotope ratios

Andreas Fichtner [a,*], Maarten De Wit [b], Manfred van Bergen [a]

[a] Department of Earth Sciences, Utrecht University, Budapestlaan 4, Utrecht 3584 CD, The Netherlands
[b] AEON and Department of Geological Sciences, University of Cape Town, Rondebosch 7700, South Africa

ARTICLE INFO

Article history:
Received 25 March 2010
Received in revised form 24 June 2010
Accepted 24 June 2010
Available online 22 July 2010

Editor: T.M. Harrison

Keywords:
continental subduction
continental lithosphere
seismic waveform tomography
isotope ratios
Banda Arc
Australia

ABSTRACT

We provide new insight into the subduction of old continental lithosphere to depths of more than 100 km beneath the Banda arc, based on a spatial correlation of full waveform tomographic images of its lithosphere with He, Pb, Nd and Sr isotope signatures in its arc volcanics. The thickness of the subducted lithosphere of around 200 km coincides with the thickness of Precambrian lithosphere as inferred from surface wave tomography. While the deep subduction of continental material in continent–continent collisions is widely recognised, the analogue process in the arc–continent collision of the Banda region is currently unique. The integrated data suggest that the late Jurassic ocean lithosphere north of the North Australian craton was capable of entraining large volumes of continental lithosphere. The Banda arc example demonstrates that continental lithosphere in arc–continent collisions is not generally preserved, thus increasing the complexity of tectonic reconstructions. In the particular case of Timor, the tomographic images indicate that this island is not located directly above the northern margin of the North Australian craton, and that decoupled oceanic lithosphere must be located at a considerable distance north of Timor, possibly as far north as the northern margin of the volcanically extinct arc sector. The tomographic images combined with isotope data suggest that subduction of the continental lithosphere did not lead to the delamination of its complete crust. A plausible explanation involves delamination within the continental crust, separating upper from lower crustal units. This interpretation is consistent with the existence of a massive accretionary complex on Timor island, with evidence from Pb isotope analysis for lower-crust involvement in arc volcanism; and with the approximate gravitational stability of the subducted lithosphere as inferred from the tomographic images. The subduction of continental lithosphere including crustal material beneath the Banda arc indicates that global injection rates of continental material into the mantle may have been underestimated and that continental subduction in arc–continent collisions may have contributed more to isotopic signatures of Earth's mantle than previously recognised.

1. Introduction

The Banda arc, located near the triple junction of the Eurasian, Australian and Pacific plates is the prime example of a recent active arc–continent collision. It is distinguished by its complex neotectonic setting (Fig. 1). The 180° curvature of the arc results from the presence of two subduction zones dipping in nearly opposite directions (Cardwell and Isacks, 1978; Das, 2004): along the Timor trough the Australian plate subducted northwards beneath Eurasia until the initiation of the arc–continent collision around 5 Ma (Bowin et al., 1980; Hall, 2002). This led to the mid-Pleistocene formation of the southward-dipping Wetar thrust (McCaffrey, 1996) that accommodates most of the present-day convergence. In the north-eastern part of the arc, along the Seram trough, the Pacific plate subducts in the southwestern direction beneath Eurasia. Whether both slabs are connected or not is a matter of ongoing research (e.g. Milsom, 2001; Das, 2004)

The recent improvement in station coverage and the development of full waveform tomography (FWT) (Tape et al., 2009; Fichtner et al., 2009, 2010) now allow us to image the upper-mantle structure beneath the Banda arc in great detail. FWT accurately models and exploits complete seismic waveform information and therefore yields tomographic images that are more realistic and better resolved. We performed a FWT for the Australasian upper mantle, including the North Australian craton and the Banda arc region (Fichtner et al., 2010). This offers the opportunity to investigate the detailed structure of this young collision zone, and in particular the extent to which continental lithosphere has been subducted.

Over the past two decades ample evidence has been presented for the subduction of continental crust beneath the southern part of the Banda arc: McBride and Karig (1987) used gravity data to infer the

* Corresponding author. Tel.: +31 30 253 5948.
E-mail addresses: fichtner@geo.uu.nl (A. Fichtner), dewit@uct.ac.za (M. De Wit), vbergen@geo.uu.nl (M. van Bergen).

0012-821X/$ – see front matter © 2010 Elsevier B.V. All rights reserved.
doi:10.1016/j.epsl.2010.06.042

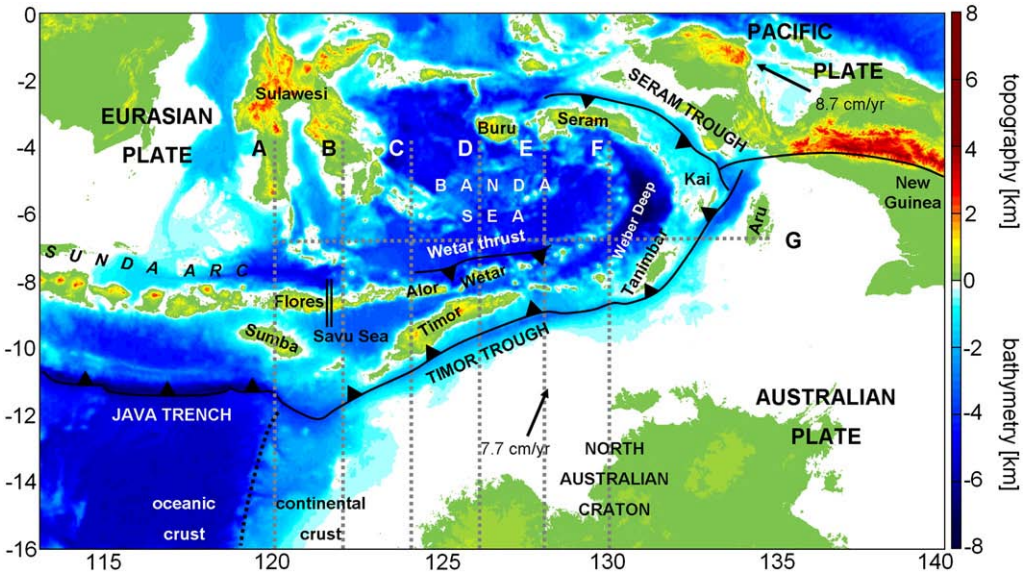

Fig. 1. Tectonic setting of the study region with topographic data from ETOPO1 (Amante and Eakins, 2009) and trench locations after Bird (2003). Arrows indicate the velocities of the Pacific and Australian plates with respect to the Eurasian plate (DeMets et al., 1994). We omit plate-motion vectors associated to the numerous micro-plates of the wider Banda Sea region. The double line across Flores marks the east–west transition from high $^3He/^4He$ ratios ($\approx 8R_A$) to low $^3He/^4He$ ratios ($\approx 1R_A$), respectively, where R_A is the helium isotope ratio of air (Hilton and Craig, 1989; Hilton et al., 1992). Gray dashed lines correspond to the velocity profiles shown in Fig. 3. For clarity we include the eastern Sunda arc islands between Alor and Timor when referring to the Banda arc.

subduction of Australian continental crust and the presence of a mass deficit in the upper mantle under the Savu Sea. Based on the observation of coda waves, Kennett and Furumura (2008) conjectured that the continental crust of the North Australian craton is adjacent to the earthquake zone beneath the Banda arc. Measurements of Sr, Nd and Pb isotopic ratios along the eastern part of the Sunda–Banda arc system exhibit clear continental signatures, suggesting the involvement of continental material in magma generation processes (e.g. Vroon et al., 1993; Elburg et al., 2004, 2005). The helium isotope ratio $R = {}^3He/{}^4He$ provides the most unequivocal and clearest evidence for the subduction of continental material beneath the Banda arc. In the western part of Flores, R increases abruptly from around 1–2 times the He ratio of air (R_A) in the Banda arc to around 6–9R_A in most of the Sunda arc, where purely oceanic material is being subducted (Hilton and Craig, 1989; Hilton et al., 1992). The inference of continental crust subduction, as opposed to subduction of continent-derived sediments alone, is based on the combination of isotope data and mass-balance calculations (van Bergen et al., 1993). Furthermore, sedimentary material is unlikely to have retained sufficient He to generate the high concentrations observed in the arc volcanics (Hilton et al., 1992). Using Pb isotope data, Elburg et al. (2004) argue for the contribution of upper as well as lower continental crust to such arc volcanism.

The data used to infer structure and composition have different resolution capabilities. Isotope ratios and gravity data have limited depth resolution, and the subcontinental lithosphere does not provide unequivocally distinctive isotopic signatures. Tomography is not capable of imaging a thin layer of subducted crust and it discriminates poorly between oceanic and continental material. These limitations motivate the principal objectives of this study: (1) improve the spatio-compositional resolution beneath the Banda arc region through the joint interpretation of isotope data and FWT images in general, and (2) determine the extent to which subcontinental lithosphere is being subducted. This is intended to further our understanding of arc–continent collisions that play a major role in the growth and destruction of continental crust, the origin of mantle isotopic signatures, paleogeographic reconstructions and the formation of mountain belts and mineral deposits.

2. Full waveform tomography

Our full waveform tomography is based on the numerical solution of the elastic wave equation using a spectral-element method that operates in a spherical section (Fichtner et al., 2009). The accuracy of the solution for heterogeneous Earth models ensures that differences between observed and synthetic waveforms are primarily the result of undiscovered Earth structure and not of approximation errors. We implement a long wavelength equivalent model of the crust derived from crust 2.0 (Bassin et al., 2000), thus eliminating the need for crustal corrections (Fichtner and Igel, 2008). The crustal part of the model is also updated during the inversion. This reduces the effect of potential inaccuracies in the initial crustal model.

Our data set consists of 2137 three-component recordings from permanent stations operated by Geoscience Australia, IRIS and GEOSCOPE and from temporary networks operated by The Australian National University. We manually select time windows where the observed waveforms show a clear correspondence to the synthetics. The resulting set of waveforms comprises fundamental- and higher-mode surface waves, long-period body waves and unidentified phases. The periods of the waveforms range between 200 s and 30 s, thus ensuring that structure to depths of around 350 km can be resolved. To quantify waveform differences, we measure time- and frequency-dependent phase misfits (Fichtner et al., 2008). These are then minimised using an adjoint method based conjugate gradient algorithm.

After 19 iterations we obtained our preferred model, shown in Figs. 2 and 3. The iterative improvement of the tomographic model leads to the recovery of realistic absolute velocities that are necessary for the accurate prediction of the seismic waveforms. The resolution of the tomographic images, estimated from a series of synthetic inversions, is around 3° laterally and 40 km vertically, despite the location of the study area near the northern boundary of the model. This results, to some degree, from the large lateral extent of the waveform sensitivity kernels that allow us to improve resolution in areas off the geometric ray path. Another important diagnostic for the reliability of the tomographic images is the remarkable fit between the observed and synthetic seismograms in the complete period range from 200 s to 30 s (Fichtner et al., 2010).

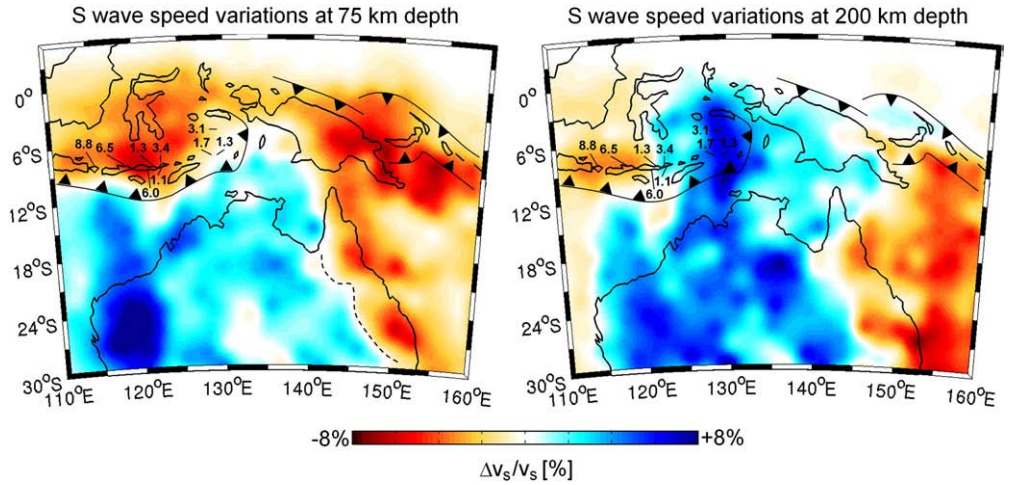

Fig. 2. Horizontal slices through the isotropic S wave speed model at 75 km and at 200 km depth. Superimposed are the positions of major faults and a selection of He isotope ratios as reported by Hilton and Craig (1989) and Hilton et al. (1992). The dashed curve in the left figure indicates the approximate depth continuation of the Tasman Line which marks the transition from Precambrian to Phanerozoic Australia. The background S wave speed is 4.39 km/s at 75 km depth and 4.53 km/s at 200 km depth.

The FWT incorporates multi-frequency information from all types of seismic waves and can be considered an extension of previous tomographic studies based on the arrival times of body waves (e.g. Widiyantoro and van der Hilst, 1996; Bijwaard et al., 1998) or surface waves (e.g. Yoshizawa and Kennett, 2004; Fishwick et al., 2005). As a result, both vertical and horizontal resolutions are high in the uppermost mantle. In particular we reduce the vertical smearing in the upper 300 km that occurs in body wave tomography as a consequence of rays pointing predominantly downdip. Further improvements of the full waveform tomographic images could come from the incorporation of seismic phases that are particularly sensitive to sharp boundaries (e.g. Ni et al., 2002; Chen et al., 2007) such as the interface between the subducted slab and the surrounding mantle. However, a sufficiently dense station coverage is currently not available in the Banda arc region. Our results and interpretation therefore depend critically on the resolution capabilities of FWT.

3. Results

Fig. 2 shows horizontal slices through the distribution of the isotropic S wave speed at 75 km and at 200 km depth beneath northern Australia and the Banda arc region. Superimposed is a selection of He isotope ratios as reported by Hilton and Craig (1989) and Hilton et al. (1992). At 75 km depth, the West and North Australian cratons can be identified by their high seismic velocities that are mostly the result of lower than average temperatures within the Precambrian lithosphere (Goes et al., 2005). The high velocities of the Precambrian cratons are bounded to the north by the Timor trough that marks the collision zone between the Australian continent and the Banda arc. The Banda Sea region including the arc is characterised by low S wave speeds around 75 km depth. Towards the east, the depth continuation of the Tasman Line (Fig. 2, left) separates high-velocity Precambrian lithosphere from low-velocity Phanerozoic lithosphere. Similar results have been found in several tomographic studies (e.g. Zielhuis and van der Hilst, 1996; Yoshizawa and Kennett, 2004; Fishwick et al., 2005).

At 200 km depth the penetration of high-velocity material northwards beyond the Timor trough is clearly visible. This feature was not part of the initial model (see Fichtner et al., 2009), and it appeared during the first iterations, thus indicating that it is required by the data. A similar, though less pronounced structure can be found in the tomographic models of Debayle and Kennett (2000), Debayle et al. (2005), Fishwick et al. (2008) and Fishwick and Reading (2008). The high velocity beneath the Banda Sea can be associated to lower-than average temperatures because thermal effects dominate over compositional effects in the uppermost mantle (e.g. Piazzoni et al., 2007). The presence of cold and brittle material around 200 km depth beneath the Banda Sea is consistent with the occurrence of intermediate-size earthquakes around the same depth in that region (Das, 2004).

On horizontal length scales of around 300 km and above 350 km depth, the geometry of the seismic velocity heterogeneities beneath northern Australia and the Banda Sea agrees well with the results of Widiyantoro and van der Hilst (1996). However, a significant difference between the full waveform tomographic model and images of slab structure obtained from teleseismic body wave tomography is the amplitude of the velocity perturbations. Velocity variations in body wave tomography (e.g. Widiyantoro and van der Hilst, 1996; Bijwaard et al., 1998) are on the order of $\pm 1.5\%$ compared to $\pm 8\%$ for the model shown in Figs. 2 and 3. This discrepancy results from the iterative improvement of the full waveform tomographic images that proceeds until the variations are sufficiently large to explain the complete observed waveforms.

We observe a remarkable and previously unrecognised coincidence of transitions in He, Pb, Sr and Nd isotope ratios (e.g. Hilton et al., 1992; Vroon et al., 1993; Elburg et al., 2005) in eastern Flores with the transition from lower wave speeds beneath the eastern Sunda arc to higher wave speeds beneath the Banda arc. This coincidence must be understood within about 3° lateral resolution and it supports the direct transfer of compositional information from isotope measurements into the tomographic images. Low He isotope ratios (≈ 1.0–$3.4 R_A$) combined with He abundances (Hilton et al., 1992) and the isotope signatures of Pb, Sr and Nd (e.g. Vroon et al., 1993; Elburg et al., 2004, 2005) are consistent with the presence of continental crust at more than 100 km depth beneath the Banda arc. This suggests the association of the high-velocity material with continental rather than oceanic lithosphere. The predominance of oceanic lithosphere, and thus of oceanic crust, would result in He isotope ratios around 6.0–$8.0 R_A$, as are typically found along circum-Pacific arcs and the Sunda arc east of the He transition (Poreda and Craig, 1989).

Vertical cross-sections through the tomographic model are presented in Fig. 3. Black triangles mark the position of the Timor trough and thin arrows indicate the positions of arc islands where He isotope ratios were measured (Hilton et al., 1992). As an aid to the interpretation of the images with limited lateral resolution ($\approx 3°$) we superimpose the positions of earthquake hypocentres for the years 2000–2009, taken from the catalogue of the National Earthquake Information Center (NEIC). At 120°E, i.e. west of the He transition

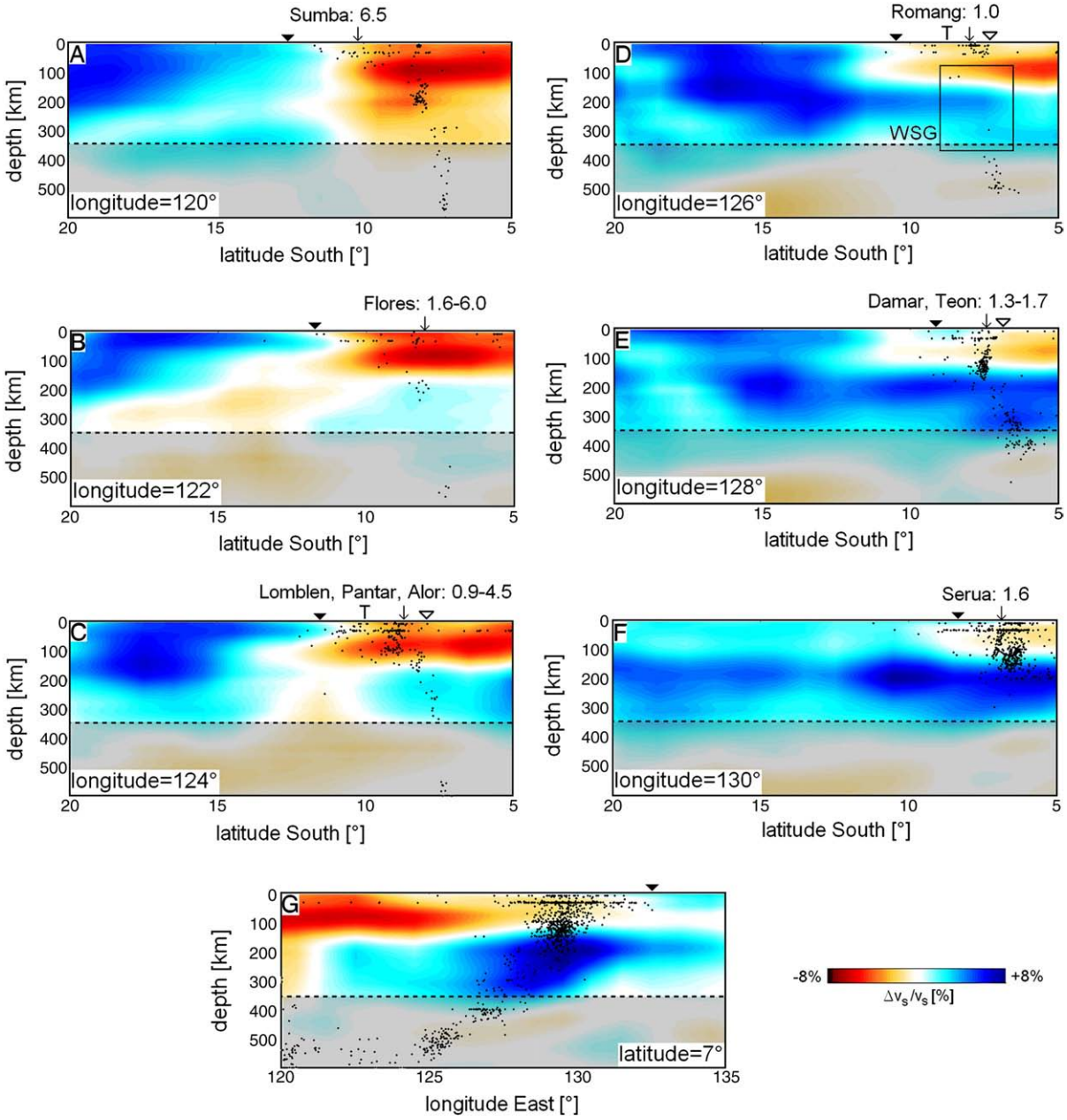

Fig. 3. Vertical slices through the isotropic S wave speed model at constant longitudes (A–F) and constant latitude (G), as indicated by gray dashed lines in Fig. 1. Tomographic resolution is insufficient north of 5°S and in the shaded regions below 350 km depth. Black filled triangles mark the position of the Timor trough, and the position of the Wetar thrust is indicated by empty triangles. Thin arrows point to Banda arc islands that are located within $\pm 1°$ of a given longitude. Numbers indicate ranges of He isotope ratios as reported by Hilton and Craig (1989) and Hilton et al. (1992). The position of the island of Timor is marked by a capital T. As an interpretative aid we superimpose earthquake hypocentres for the years 2000–2009 taken from the catalogue of the National Earthquake Information Center (NEIC). These are plotted a black dots. The low-seismicity zone known as Wetar Seismic Gap (WSG) (e.g. Das, 2004; Ely and Sandiford, 2010) is indicated by a black quadrangle in cross-section D. The background S wave model is PREM (Dziewonski and Anderson, 1981) with the 220 km discontinuity replaced by a gradient to avoid biases in the tomographic images (Fichtner et al., 2010). The resolution of the tomographic images, estimated from a series of synthetic inversions, is around 3° laterally and 40 km vertically.

where the oceanic part of the Australian plate is being subducted, the volcanic arc is underlain by seismically slow material. The thin and steeply-dipping oceanic slab (Widiyantoro and van der Hilst, 1996) is not visible in our images that are dominated by surface wave data. It can, however, be traced with the help of hypocentre locations. Slightly east of the He transition, at 122°E, seismically fast material appears at depths greater than 200 km beneath the arc. Isotopic signatures of Pb and He again indicate the presence of continental crust at magmagenic depth (e.g. Hilton et al., 1992; Elburg et al., 2004, 2005), thus suggesting the interpretation of the high-velocity material in terms of the associated continental lithosphere.

From 122°E to 124°E, the lithosphere south of the trench and the subducted lithosphere beneath the arc are interrupted by low-velocity material. The horizontal slices in Fig. 2 show that this gap is the result of a low-velocity indenter near 120°E that extends from beneath Sumba southwards across the trench. This geometric complexity may be related to the transition from the steep subduction of oceanic lithosphere (Widiyantoro and van der Hilst, 1996) to the shallow subduction of the North Australian margin.

With increasing longitude, the high-velocity region beneath the arc becomes increasingly pronounced and it connects to the high velocities of the North Australian craton east of 125°E. The high-

velocity material reaches about 300 km depth. Its thickness of around 200 km is similar to the seismologically inferred thickness of Precambrian lithosphere under Australia (e.g. Zielhuis and van der Hilst, 1996; Fishwick et al., 2005; Fichtner et al., 2009) thus supporting our interpretation in terms of continental lithosphere. Around 126° we observe that high seismic velocities coincide with the Wetar seismic gap (e.g. Das, 2004; Ely and Sandiford, 2010) — a region between 100 and 400 km depth that is marked by the nearly complete absence of seismicity. North of the arc, high-velocity material appears to underlie most of the Banda Sea nearly horizontally. A transition from the thick continental lithosphere to thinner oceanic lithosphere is not observable south of 5°S where the resolution starts to become poor towards the north. West of 126°E the tomographic images are influenced by both the northward subduction along the Timor trough and the westward subduction along the Seram trough. This renders the unambiguous association of high seismic wave speeds west of 126°E to one of the slabs nearly impossible.

4. Discussion

Our interpretation of higher than average seismic velocities beneath the Banda arc in terms of subducted continental lithosphere is based on a unique geographic correlation between isotope signatures and tomographic images. Isotope ratios and abundances of He, Pb, Sr and Nd east of Flores suggest the presence of upper and possibly lower continental crust at magmagenic depth (e.g. Hilton et al., 1992; Elburg et al., 2004, 2005). The associated subcontinental lithosphere is clearly visible in the tomographic images in the form of high-velocity material underlying the arc below 100 km depth. The thickness of this material, around 200 km, agrees well with the thickness of the Australian Precambrian lithosphere.

4.1. Deep continental subduction in arc–continent collisions

The viability of deep continental subduction has generally been inferred from indirect observations. Most importantly, the formation of coesite, micro-diamonds and other ultrahigh-pressure index minerals in orogenic belts around the globe has been shown to require the deep subduction of continental crust (e.g. Sobolev and Shatsky, 1990; Chopin et al., 1991; Wang et al., 1992; Xu et al., 1992; Dobrzhinetskaya et al., 1995; Chopin and Sobolev, 1995; Massonne, 1999). Continental subduction into the garnet stability field of the overlying mantle wedge has been proposed as a possible mechanism for the crustal emplacement of orogenic garnet peridotites (Brueckner, 1998; Brueckner and Medaris, 2000). Garnet peridotites in the Western Gneiss Region, SW Norway, indicate the subduction of continental crust to depths of 180–200 km (Spengler et al., 2009). Additional evidence for similarly deep subduction of continental material is provided by exsolutions of clinopyroxene, rutile and apatite in garnet. These have been observed, for example, in the Sulu ultrahigh-pressure belt, China (Ye et al., 2000) and the Northern Tibetan Plateau (Song et al., 2004).

The subduction of continental crust in continent–continent collisions is now widely recognised. However, the large-scale subduction of complete continental lithosphere beneath the Banda arc is at present a globally unique feature in arc–continent collisional settings. There is no evidence for a similar tectonic process in the currently active arc–continent collision near Taiwan (e.g. Wang et al., 2006; Huang et al., 2006) or the late Paleocene to middle Miocene arc–continent collision in the Caribbean (Gordon et al., 1997; Godey et al., 2004). This is surprising despite the inherent complexity of collisions that prohibits their direct comparison.

4.2. Implications for plate tectonic reconstructions

Tomographic images are central in plate tectonic reconstructions of regions, such as Southeast Asia, that are marked by non-rigid deformation, moving plate boundaries and the rapid subduction of micro-plates (e.g. Hall, 2002). An immediate implication of Figs. 2 and 3 is that the lateral extent of continental lithosphere should not be assumed to be near-preserved during arc–continent collisions. The possible violation of this preservation hypothesis adds considerable uncertainty to reconstructions of past arc–continent collisions in orogenic belts including the Urals, the Appalachians, and the Alpine–Himalayan chain.

4.3. The role of the crust: Subduction and delamination

The combined evidence from tomographic images and isotope ratios indicates the presence of continental crust at depths between 100 and 150 km beneath the Banda arc. The late Jurassic ocean lithosphere, that existed north of the Australian continent, was thus permitting subduction of comparatively light continental crust into the denser uppermost mantle against the action of buoyancy forces.

Experimental data (Irifune et al., 1994) show that continental crust above 300 km depth is less dense than the surrounding mantle and therefore buoyant. There are, however, indicators for an approximate gravitational stability of the continental lithosphere in the Banda Sea region. These include the existence of the Banda Sea itself and the nearly horizontal position of the high-velocity material seen in Fig. 3. Based on numerical models, Capitanio et al. (2010) hypothesise that continental lithosphere may become denser when the upper crust is scraped off during the collision process, possibly leading to the deep subduction of continental lithosphere beneath the Himalayan orogen. While this scenario remains contestable in the specific context of the India–Asia convergence (Müller, 2010) it appears plausible in the Banda arc region where a partial disintegration of upper-crustal material is supported by the contribution of lower-crustal material to magmatism as inferred from Pb isotope data (Elburg et al., 2004) and where ample evidence exists for massive accretionary addition of the uppermost part of continental-margin material onto the overriding plate (e.g. Hamilton, 1979; Charlton et al., 1991).

Our results suggest that the subduction of the continental lithosphere did not lead to the complete delamination of the crust along a rheological weak zone flanking the Moho (Kohlstedt et al., 1995) as observed in other orogenic belts (e.g. Bird, 1978). We propose three explanations for the absence of complete crustal delamination: (1) The most plausible scenario involves delamination within the continental crust, thus separating upper from lower crustal units. This interpretation, also suggested by various tectonic models (e.g. Audley-Charles, 2004), is consistent with evidence from Pb isotope analysis for lower-crust involvement in the Banda arc volcanism (Elburg et al., 2004). (2) The shallow subduction angle may have prevented the occurrence of sufficiently high shear stress at the base of the crust. (3) Low geothermal gradients may have shifted the brittle–ductile transition to greater depth and possibly below the Moho (Cull, 1989). Sufficiently low heat flow values around 40 mW m^{-2} have been reported for north and western Australia (Cull, 1982).

4.4. Slab detachment and the Wetar Seismic Gap

The arc segment between 125°E and 128°E is marked by relatively rapid uplift ($\approx$0.5–1.0 m per 1000 years; e.g. Chappell and Veeh, 1978), the absence of active volcanism (e.g. Elburg et al., 2004, 2005) and the pronounced Wetar seismic gap that is clearly visible in Fig. 3 (e.g. Das, 2004). These observations have been taken as evidence for the detachment of the oceanic slab from the continental lithosphere, and the seismic gap was interpreted in terms of a slab window (e.g. Ely and Sandiford, 2010).

However, the tomographic images (Figs. 3 and 2) do not indicate the presence of an extended slab window where seismic velocities would be expected to be lower than average. Instead, the location of

the Wetar seismic gap coincides with a region of higher than average seismic velocities, in agreement with previous body wave tomographic studies (e.g. Widiyantoro and van der Hilst, 1996; Bijwaard et al., 1998). Since a nearly 300 km wide slab window is expected to be tomographically resolvable, we conjecture that the low seismicity is not likely due to the absence of oceanic lithosphere along the entire depth range from 100 km to 400 km.

The tomographic images combined with the isotope data suggest that a slab detachment may have occurred below 250 km depth and that the presence of nearly neutrally buoyant continental lithosphere may contribute to the low seismic activity.

4.5. Implications for the origin of Timor

Concerning the outer Banda arc islands, and Timor in particular, we infer that they are not located directly above the northern edge of the North Australian craton, as suggested in various paleogeographic models (e.g. Lee and Lawver, 1995; Hall, 2002). This follows already from the isotope ratios measured along the inner arc (e.g. Hilton et al., 1992; van Bergen et al., 1993) that were, however, not previously incorporated into tectonic reconstructions.

The tomographic images favour scenarios where sequences of the Australian margin, found on Timor, have been tectonically stacked in an evolving accretionary complex (e.g. Hamilton, 1979; Charlton et al., 1991). Yet, they do not necessarily exclude tectonic models where the formation of Timor and its rapid late Neogene uplift are associated with oceanic slab break-off followed by rebound of the continental margin (e.g. Price and Audley-Charles, 1987; Charlton, 1991). However, decoupling of oceanic lithosphere should be located at a considerable distance north of Timor, in line with seismological evidence for slab rupture beneath the volcanic arc (Sandiford, 2008) and for recent strong uplift as far north as the northern margin of the volcanically extinct arc sector (Hantoro et al., 1994). Furthermore, it remains to be assessed how much of the crustal uplift is attributable to lithospheric deformation which likely plays a role as well, e.g. since late Quaternary surface uplift rates are not evenly distributed but vary more than an order of magnitude along and across the emerging Banda Arc orogen (Merritts et al., 1998).

4.6. Relation to mantle isotope signatures

It remains uncertain to what degree the large-scale subduction of continental lithosphere observed today in the Banda arc system is representative of the time span during which plate tectonics operated. Nevertheless, its current existence indicates that the recycling rates of continental material into the mantle along arc–continent collision zones may have been underestimated. These estimates mostly assume that the subduction of sediments and subduction erosion dominate the flux of continental material into the mantle along arc–continent collisions (e.g. Clift et al., 2009). While this assumption may be valid in cases such as Taiwan where neither isotope nor tomographic evidence for the deep subduction of continental lithosphere exist (e.g. Wang et al., 2006), it does not hold in the Banda arc. A meaningful quantification of the amount of continental crust subducted into the mantle along the Banda arc will require a more detailed tomographic study based on local data that are currently not available.

5. Conclusions

We combine tomographic images and isotope data to improve the spatio-compositional resolution in the upper-mantle beneath the Banda Sea region. A strong correlation exists between He, Pb, Nd and Sr isotope signatures of arc volcanics (e.g. Hilton et al., 1992; Vroon et al., 1993; Elburg et al., 2005) and seismic velocities below 100 km depth. This correlation has not been recognised before and it supports the transfer of geochemical information from isotopes into the seismic tomographic images. In particular, low $^3He/^4He$ ratios around $1–2R_A$ along the Banda arc east of Flores (e.g. Hilton et al., 1992) suggest the association of high-velocity material below 100 km with subducted continental lithosphere. The thickness of subducted high-velocity material, around 200 km, agrees with the thickness of Precambrian Australian lithosphere as inferred from seismic tomography (e.g. Zielhuis and van der Hilst, 1996; Yoshizawa and Kennett, 2004; Fishwick et al., 2005; Fichtner et al., 2009). While the deep subduction of continental material is today widely recognised in continent–continent collisions (e.g. Sobolev and Shatsky, 1990; Ye et al., 2000; Spengler et al., 2009) the analogue process in the arc–continent collision of the Banda region is currently unique.

Major conclusions drawn from the subduction of continental lithosphere beneath the Banda arc are: (1) The late Jurassic ocean lithosphere north of Australia permitted the subduction of large volumes of continental lithosphere including crustal material to depths below 100 km. (2) Tomographic images and the existence of the Banda Sea suggest that the subducted continental lithosphere is nearly neutrally buoyant. The partial tectonic removal of upper-crustal material, supported by Pb isotope data in the volcanic arc (Elburg et al., 2004) and by the existence of a massive accretionary complex, may explain this observation. (3) The lateral extent of continental lithosphere is not generally preserved in arc–continent collisions, as often assumed in tectonic reconstructions (e.g. Lee and Lawver, 1995; Hall, 2002). (4) The Wetar seismic gap coincides with a region of higher than average velocities. A slab window resulting from oceanic slab detachment is therefore unlikely to fully explain the relative seismic quiescence in the complete depth range from 100 km to 400 km. (5) The island of Timor is not located directly above the northern margin of the North Australian craton. This argues for tectonic models where decoupling of oceanic lithosphere is located as far north as the northern margin of the volcanically extinct arc sector. (6) The injection rates and the degree of recycling of continental material into the mantle may be underestimated because the possible continental subduction along arc–continent collisions is not taken into account (e.g. Clift et al., 2009).

Our interpretation depends critically on the resolution capabilities of FWT that result from the use of multi-frequency information from all types of seismic waves including surface and body waves. Nevertheless, more detailed tomographic studies involving local data are necessary to obtain a more complete picture and in particular to quantify the amount of continental lithosphere subducted beneath the Banda arc.

Acknowledgements

The authors would like to thank Hans-Peter Bunge for the initiation of this collaboration. We are particularly grateful to Rocco Malservisi, Brian Kennett, Jeannot Trampert, Hanneke Paulssen, Wim Spakman and Rob Govers for discussions that helped us to improve the manuscript. The data used in this study were provided by Iris, GEOSCOPE, Geoscience Australia and the temporary networks operated by the Research School of Earth Sciences at the Australian National University. We thank Armando Arcidiaco, Agus Abdullah, Stewart Fishwick and Hrvoje Tkalčić for their help with the temporary network data and the station responses. The high-performance computations for the solution of the waveform tomographic problem would not have been possible without the support of the Leibniz Rechenzentrum in Garching. Many thanks also to Jens Oeser for creating a unique computing infrastructure at the Institute of Geophysics at Munich University. The constructive criticism of Carl Tape, Stewart Fishwick and an anonymous reviewer allowed us to substantially improve the manuscript. This is AEON contribution number 80.

References

Amante, C., Eakins, B. W., 2009. ETOPO1 1 Arc-Minute Global Relief Model: Procedures, Data Sources and Analysis. NOAA Technical Memorandum NESDIS NGDC-24, 19 pp.

Audley-Charles, M.G., 2004. Ocean trench blocked and obliterated by Banda forearc collision with Australian proximal continental slope. Tectonophysics 389, 65–79.

Bassin, C., Laske, G., Masters, G., 2000. The current limits of resolution for surface wave tomography in North America. EOS Trans. AGU 81, F897.

Bijwaard, H., Spakman, W., Engdahl, E.R., 1998. Closing the gap between regional and global travel time tomography. J. Geophys. Res. 103, 30055–30078.

Bird, P., 1978. Initiation of intracontinental subduction in the Himalaya. J. Geophys. Res. 83, 4975–4987.

Bird, P., 2003. An updated digital model of plate boundaries. Geochemistry Geophysics Geosystems 4 (3), doi:10.1029/2001GC000252.

Bowin, C., Purdy, G.M., Johnston, C., Shor, G., Lawver, L., Hartono, H.M.S., Jezek, P., 1980. Arc–continent collision in the Banda Sea region. AAPG Bull. 64, 868–915.

Brueckner, H.K., 1998. Sinking intrusion model for the emplacement of garnet-bearing peridotites into continent collision orogens. Geology 26, 631–634.

Brueckner, H.K., Medaris, L.G., 2000. A general model for the intrusion and evolution of mantle garnet peridotites in high-pressure and ultrahigh-pressure metamorphic terranes. J. Metamorph. Geol. 18, 123–133.

Capitanio, F.A., Morra, G., Goes, S., Weinberg, R.F., Moresi, L., 2010. India–Asia convergence driven by the subduction of the Greater Indian continent. Nat. Geosci. 3, 136–139.

Cardwell, R.K., Isacks, B.L., 1978. Geometry of the subducted lithosphere beneath the Banda Sea in eastern Indonesia from seismicity and fault plane solutions. J. Geophys. Res. 83, 2825–2838.

Charlton, T.R., 1991. Postcollisional extension in arc–continent collision zones, eastern Indonesia. Geology 19, 28–31.

Charlton, T.R., Barber, A.J., Barkham, S.T., 1991. The structural evolution of the Timor collision complex, eastern Indonesia. J. Struct. Geol. 13, 489–500.

Chappell, J., Veeh, H.H., 1978. Late Quaternary tectonic movements and sea-level changes at Timor and Atauro island. Geol. Soc. Am. Bull. 89, 356–368.

Chen, M., Tromp, J., Helmberger, D., Kanamori, H., 2007. Waveform modelling of the slab beneath Japan. J. Geophys. Res. 112. doi:10.1029/2006JB004394.

Chopin, C., Henry, C., Michard, A., 1991. Geology and petrology of the coesite-bearing terrain, Dora-Maira Massif, Western Alps. Eur. J. Mineral. 3, 263–291.

Chopin, C., Sobolev, N.V., 1995. Principal mineralogical indicators of ultrahigh pressure in crustal rocks. Ultrahigh Pressure Metamorphism. Cambridge University Press, pp. 96–131.

Clift, P.D., Vannucchi, P., Morgan, J.P., 2009. Crustal redistribution, crust–mantle recycling and Phanerozoic evolution of the continental crust. Earth-Sci. Rev. 97, 80–104.

Cull, J.P., 1982. An appraisal of Australian heat-flow data. BMR J. Aust. Geol. Geophys. 7, 11–21.

Cull, J.P., 1989. Geothermal models and mantle rheology in Australia. Tectonophysics 164, 107–115.

Das, S., 2004. Seismicity gaps and the shape of the seismic zone in the Banda Sea region from relocated hypocenters. J. Geophys. Res. 109. doi:10.1029/2004JB003192.

Debayle, E., Kennett, B.L.N., 2000. The Australian continental upper mantle: structure and deformation inferred from surface waves. J. Geophys. Res. 105, 25423–25450.

Debayle, E., Kennett, B.L.N., Priestley, K., 2005. Global azimuthal seismic anisotropyand the unique plate motion deformation of Australia. Nature 433, 509–512.

DeMets, C., Gordon, R.G., Argus, D.F., Stein, S., 1994. Effect of recent revisions to geomagnetic reversal time scale on estimates of current plate motions. Geophys. Res. Lett. 21, 2191–2194.

Dobrzhinetskaya, L.F., Eide, E.A., Larsen, R.B., Sturt, B.A., Tronnes, R.G., Smith, D.C., Taylor, W.R., Posukhova, T.V., 1995. Microdiamond in high-grade metamorphic rocks of the Western Gneiss Region, Norway. Geology 23, 597–600.

Dziewonski, A.M., Anderson, D.L., 1981. Preliminary reference Earth model. Phys. Earth Planet. Inter. 25, 297–356.

Elburg, M.A., van Bergen, M.J., Foden, J.D., 2004. Subducted upper and lower continental crust contributes to magmatism in the collision sector of the Sunda–Banda arc, Indonesia. Geology 32, 41–44.

Elburg, M.A., Foden, J.D., van Bergen, M.J., Zulkarnain, I., 2005. Australia and Indonesia in collision: geochemical sources of magmatism. J. Volcanol. Geother. Res. 140, 25–47.

Ely, K.S., Sandiford, M., 2010. Seismic response to slab rupture and variation in lithospheric structure beneath the Savu Sea. Tectonophysics 483, 112–124.

Fichtner, A., Igel, H., 2008. Efficient numerical surface wave propagation through the optimisation of discrete crustal models — a technique based on non-linear dispersion curve matching (DCM). Geophys. J. Int. 173, 519–533.

Fichtner, A., Kennett, B.L.N., Igel, H., Bunge, H.-P., 2008. Theoretical background for continental- and global-scale full waveform inversion in the time–frequency domain. Geophys. J. Int. 175, 665–685.

Fichtner, A., Kennett, B.L.N., Igel, H., Bunge, H.-P., 2009. Full seismic waveform tomography for upper-mantle structure in the Australasian region using adjoint methods. Geophys. J. Int. 179, 1703–1725.

Fichtner, A., Kennett, B.L.N., Igel, H., Bunge, H.-P., 2010. Full waveform tomography for radially anisotropic structure: new insights into present and past states of the Australasian upper mantle. Earth Planet. Sci. Lett. 290, 270–280.

Fishwick, S., Kennett, B.L.N., Reading, A.M., 2005. Contrasts in lithospheric structure within the Australian craton — insights from surface wave tomography. Earth Planet. Sci. Lett. 231, 163–176.

Fishwick, S., Heintz, M., Kennett, B.L.N., Reading, A.M., Yoshizawa, K., 2008. Steps in lithospheric thickness within eastern Australia, evidence from surface wave tomography. Tectonics 27 (4), TC0049. doi:10.1029/2007TC002116.

Fishwick, S., Reading, A., 2008. Anomalous lithosphere beneath the Proterozoic of western and central Australia: a record of continental collision and intraplate deformation? Precambrian Res. 166, 111–121.

Godey, S., Deschamps, F., Trampert, J., Snieder, R., 2004. Thermal and compositional anomalies beneath the North American continent. J. Geophys. Res. 109, B01308. doi:10.1029/2002JB002263.

Goes, S., Simons, F.J., Yoshizawa, K., 2005. Seismic constraints on temperature of the Australian uppermost mantle. Earth Planet. Sci. Lett. 236, 227–237.

Gordon, M.B., Mann, P., Caceres, D., Flores, R., 1997. Cenozoic tectonic history of the North America-Caribbean plate boundary zone in western Cuba. J. Geophys. Res. 102, 10,055–10,082.

Hall, R., 2002. Cenozoic geological and plate tectonic evolution of SE Asia and the SW Pazific: computer-based reconstructions, model and animations. J. Asian Earth Sci. 20, 353–431.

W. Hamilton, 1979. Tectonics of the Indonesian Region. USGS Paper 1078.

Hantoro, W.S., Pirazzoli, P.A., Jouannic, C., Faure, H., Hoang, C.T., Radtke, U., Causse, C., Borel Best, M., Lafont, R., Bieda, S., Lambeck, K., 1994. Quaternary uplifted coral reef terraces on Alor Island, East Indonesia. Coral Reefs 13, 215–223.

Hilton, D.R., Craig, H., 1989. A helium isotope transect along the Indonesian archipelago. Nature 342, 906–908.

Hilton, D.R., Hoogewerff, J.A., van Bergen, M.J., Hammerschmidt, K., 1992. Mapping magma sources in the east Sunda–Banda arc, Indonesia: constraints from helium isotopes. Geochim. Cosmochim. Acta 56, 851–859.

Huang, C.-Y., Yuan, P.B., Tsao, S.-J., 2006. Temporal and spatial records of active arc–continent collision in Taiwan: a synthesis. Geol. Soc. Am. Bull. 118, 274–288.

Irifune, T., Ringwood, A.E., Hibberson, W.O., 1994. Subduction of continental crust and terrigenous and pelagic sediments: an experimental study. Earth Planet. Sci. Lett. 126, 351–368.

Kennett, B.L.N., Furumura, T., 2008. Stochastic waveguide in the lithosphere: Indonesian subduction zone to Australian craton. Geophys. J. Int. 172, 363–382.

Kohlstedt, D.L., Evans, B., Mackwell, S.J., 1995. Strength of the lithosphere: Constraints imposed by laboratory measurements. J. Geophys. Res. 100, 17,587–17,602.

Lee, T.-Y., Lawver, L.A., 1995. Cenozoic plate reconstruction of Southeast Asia. Tectonophysics 251, 85–138.

Massonne, H.J., 1999. A new occurrence of microdiamonds in quartzofeldspathic rocks of the Saxonian Erzgebirge, Germany, and their metamorphic evolution. Proceedings of the VIIth International Kimberlite Conference, Cape Town 1998, 533–539.

McBride, J.H., Karig, D.E., 1987. Crustal structure of the outer Banda arc: new free-air gravity evidence. Tectonophysics 140, 265–273.

McCaffrey, R., 1996. Slip partitioning at convergent plate boundaries of SE Asia. In: Hall, R., Blundell, D.J. (Eds.), Tectonic evolution of Southeast Asia: Geological Society of London, Special Publication, 106, pp. 3–18.

Merritts, D., Eby, R., Harris, R., Edwards, R.L., Chang, H., 1998. Variable rates of late Quaternary surface uplift along the Banda Arc–Australia plate collision zone, Eastern Indonesia. Geol. Soc. London Spec. Pub. 146, 213–224.

Milsom, J., 2001. Subduction in eastern Indonesia: how many slabs? Tectonophysics 338, 167–178.

Müller, R.D., 2010. Sinking continents. Nat. Geosci. 3, 79–80.

Ni, S., Tan, E., Gurnis, M., Helmberger, D., 2002. Sharp sides to the African superplume. Science 296, 1850–1853.

Piazzoni, A., Steinle-Neumann, G., Bunge, H.-P., Dolejs, D., 2007. A mineralogical model for density and elasticity of the Earth's mantle. Geochem. Geophys. Geosyst. 8. doi:10.1029/2007GC001697.

Poreda, R., Craig, H., 1989. Helium isotope ratios in circum-Pacific volcanic arcs. Nature 338, 473–478.

Price, N.J., Audley-Charles, M.G., 1987. Tectonic collision processes after plate rupture. Tectonophysics 140, 121–129.

Sandiford, M., 2008. Seismic moment release during slab rupture beneath the Banda Sea. Geophys. J. Int. 174, 659–671.

Sobolev, N.V., Shatsky, V.S., 1990. Diamond inclusions in garnets from metamorphic rocks. Nature 343, 742–746.

Song, S., Zhang, L., Niu, Y., 2004. Ultra-deep origin of garnet peridotite from the North Qaidam ultrahigh-pressure belt, Northern Tibetan Plateau, NW China. Am. Mineral. 89, 1330–1336.

Spengler, D., Brueckner, H.K., van Roermund, H.L.M., Drury, M.R., Mason, P.R.D., 2009. Long-lived, cold burial of Baltica to 200 km depth. Earth Planet. Sci. Lett. 281, 27–35.

Tape, C., Liu, Q.Y., Maggi, A., Tromp, J., 2009. Adjoint tomography of the Southern California crust. Science 325, 988–992.

van Bergen, M.J., Vroon, P.Z., Hoogewerff, J.A., 1993. Geochemical and tectonic relationships in the east Indonesian arc–continent collision region: implications for the subduction of the Australian passive margin. Tectonophysics 223, 97–116.

Vroon, P.Z., van Bergen, M.J., White, W.M., Varekamp, J.C., 1993. Sr–Nd–Pb isotope systematics of the Banda arc, Indonesia: Combined subduction and assimilation of continental material. J. Geophys. Res. 98, 22,349–22,366.

Wang, X.M., Liou, J.G., Maruyama, S., 1992. Coesite-bearing eclogites from the Dabie mountains, Central China — petrogenesis, P–T paths, and implications for regional tectonics. J. Geol. 100, 231–251.

Wang, Z., Zhao, D., Wang, J., Kao, H., 2006. Tomographic evidence for the Eurasian lithosphere subducting beneath south Taiwan. Geophys. Res. Lett. 33, L18306. doi:10.1029/2006GL027166.

Widiyantoro, S., van der Hilst, R.D., 1996. Structure and evolution of lithospheric slab beneath the Sunda arc, Indonesia. Science 271, 1566–1570.
Xu, S., Okay, A., Ji, S.Y., Sengor, A.M.C., Wen, S., Liu, Y.C., Jiang, L.L., 1992. Diamond from the Dabie–Shan metamorphic rocks and its implication for tectonic setting. Science 256, 80–82.
Ye, K., Cong, B., Ye, D., 2000. The possible subduction of continental material to depths greater than 200 km. Nature 407, 734–736.
Yoshizawa, K., Kennett, B.L.N., 2004. Multimode surface wave tomography for the Australian region using a three-stage approach incorporating finite frequency effects. J. Geopyhs. Res. 109. doi:10.1029/2002JB002254.
Zielhuis, A., van der Hilst, R.D., 1996. Upper-mantle shear velocity beneath eastern Australia from inversion of waveforms from SKIPPY portable arrays. Geophys. J. Int. 127, 1–16.